Received: 9 October 2021 | Revised: 27 January 2022 | Accepted: 1 March 2022

DOI: 10.1002/jev2.12204

RESEARCH ARTICLE

A new strategy to count and sort neutrophil-derived extracellular vesicles: Validation in infectious disorders

Amandine Bonifay[1,2] | **Stéphane Robert**[1] | **Belinda Champagne**[1] | **Paul-Rémi Petit**[2] | **Aude Eugène**[2] | **Corinne Chareyre**[1] | **Anne-Claire Duchez**[1] | **Mélanie Vélier**[1,2] | **Shirley Fritz**[2] | **Loris Vallier**[1] | **Romaric Lacroix**[1,2] | **Françoise Dignat-George**[1,2]

[1]Aix-Marseille University, C2VN, INSERM 1263, INRA 1260, Marseille, France

[2]Department of Hematology and Vascular Biology, CHU La Conception, APHM, Marseille, France

Correspondence
Françoise Dignat-George, Aix-Marseille University, C2VN, INSERM 1263, INRA 1260, Marseille, France.
Email: francoise.dignat-george@univ-amu.fr

Abstract

Newly recognized polymorphonuclear neutrophil (PMNs) functions include the ability to release subcellular mediators such as neutrophil-derived extracellular vesicles (NDEVs) involved in immune and thrombo-inflammatory responses. Elevation of their plasmatic level has been reported in a variety of infectious and cardiovascular disorders, but the clinical use of this potential biomarker is hampered by methodological issues. Although flow cytometry (FCM) is currently used to detect NDEVs in the plasma of patients, an extensive characterization of NDEVs has never been done. Moreover, their detection remains challenging because of their small size and low antigen density. Therefore, the objective of the present study was first to establish a surface antigenic signature of NDEVs detectable by FCM and therefore to improve their detection in biological fluids by developing a strategy allowing to overcome their low fluorescent signal and reduce the background noise. By testing a large panel of 54 antibody specificities already reported to be positive on PMNs, we identified a profile of 15 membrane protein markers, including 4 (CD157, CD24, CD65 and CD66c) never described on NDEVs. Among them, CD15, CD66b and CD66c were identified as the most sensitive and specific markers to detect NDEVs by FCM. Using this antigenic signature, we developed a new strategy combining the three best antibodies in a cocktail and reducing the background noise by size exclusion chromatography (SEC). This strategy allowed a significant improvement in NDEVs enumeration in plasma from sepsis patients and made it feasible to efficiently sort NDEVs from COVID-19 patients. Altogether, this work opens the door to a more valuable measurement of NDEVs as a potential biomarker in clinical practice. A similar strategy could also be applied to improve detection by FCM of other rare subpopulations of EVs generated by tissues with limited access, such as vascular endothelium, cancer cells or placenta.

KEYWORDS

EVs sorting, extracellular vesicles, flow cytometry, infectious associated diseases, neutrophils, size exclusion chromatography

1 | INTRODUCTION

Research in the last 10 years has uncovered a number of unexpected aspects of polymorphonuclear neutrophil (PMN) biology. Their heterogeneous features, including PMN maturity, functionality and death, have led to a reconsideration of their role in

many diseases, including inflammatory and infectious disorders (Kolaczkowska and Kubes, 2013), cardiovascular (Gaul et al., 2017) and thrombotic diseases (Kapoor et al., 2018) and cancer (Galdiero et al., 2018). Newly recognized PMN functions include the ability to release subcellular mediators such as extracellular DNA (Van Avondt and Hartl, 2018) and extracellular vesicles (EVs) (Hong, 2018) involved in immune and thrombo-inflammatory responses. Indeed, similar to other eukaryotic cells, PMNs, under basal or activated states, have been shown to generate EVs. It is now well admitted that large EVs generation is the end point of an activation cascade requiring increases in intracellular calcium concentration, the rearrangement of the cytoskeleton and the budding of these vesicles from the plasma membrane (Zwaal and Schroit, 1997). Consequently, large EVs convey a spectrum of molecules from their parent cells, including anionic phospholipids such as phosphatidylserine (PS) (Connor et al., 2010), membrane and cytosolic proteins (Choi et al., 2013) and nucleic acids (Varela-Eirin et al., 2017); however, they differ in composition, size and biogenesis from other subcellular structures, such as apoptotic bodies or small EVs (Yáñez-Mó et al., 2015). Large EVs exert biological effects by stimulating receptors of the target cell or by transferring vesicle content, such as protein, lipids, nucleic acids or organels. Large EVs display distinct molecular profiles, in vitro, according to cellular stimulation and in vivo, depending on the pathophysiological context of the disease. Additionally, it has been shown that circulating large EVs act together with soluble mediators to enhance biological processes, such as coagulation (Del Conde et al., 2005), inflammation (Headland et al., 2015) and the immune response (Cortez-Espinosa et al., 2017). Among large EVs, neutrophil-derived EVs (NDEVs) are detected in small amounts in the circulation under normal physiological conditions. However, NDEVs have been shown to accumulate at the sites of infection or inflammation (Gomez et al., 2020), and their circulating levels are elevated in a variety of infectious disorders, such as sepsis (Prakash et al., 2012), COVID-19 (Guervilly et al., 2021), atherosclerotic disorders and renal diseases, including IgA nephropathy and tubulointerstitial nephritis (Daniel et al., 2006; He et al., 2016) and in anti-neutrophil cytoplasmic antibody (ANCA)-associated vasculitis (Kambas et al., 2014).

Several studies have highlighted the relevance of NDEVs as a pertinent biomarker. Accordingly, the increase in NDEVs in plasma is correlated with disease severity and/or evolution in clinical settings such as infectious endocarditis (Guimarães Júnior et al., 2019), familial hypercholesterolaemia (Suades et al., 2019) and chronic obstructive pulmonary disease (Soni et al., 2020). Furthermore, elevated circulating NDEVs is an independent predictor of atherosclerosis burden (Martínez et al., 2017) and unstable plaque (Sarlon-Bartoli et al., 2013), and a high level of NDEVs in pleural fluids was associated with a better outcome in patients with acute respiratory distress syndrome (Guervilly et al., 2011).

Because of these clinical associations, extensive identification of the NDEVs surface molecular signature could improve our knowledge of their potential role in inflammation, infection and thrombosis and their value as a prognostic indicator of vascular diseases. This could also provide complementary tools to improve their detection in biofluids. While this is an interesting prospect, no extensive characterization of the NDEVs antigenic profile has been established to date, and the clinical use of this potential biomarker is currently hampered by methodological issues.

In the aforementioned studies, flow cytometry (FCM) is frequently used to enumerate NDEVs levels in patients. FCM appears to be the most suitable technique for the measurement of EVs in plasmatic environments for clinical application. Indeed, FCM is a multiparametric technology that provides information on a single-particle basis and offers potential for high-throughput processing. Therefore, the technology is adapted to large-scale use in most hospital laboratories. However, NDEVs detection in FCM remains challenging and is impeded by several technical issues: (1) the use of antibodies selected only according to their antigenic expression on the parental cell, (2) subcellular size of NDEVs with weak antigen density generating low fluorescent signal, (3) high fluorescent background noise generated by various confounding components including non-EVs particles and unbound reagents. Such technical issues not only hamper the enumeration of NDEVs in human plasma but also explain why NDEVs FCM sorting is currently an impractical solution and limit EV-sorting downstream applications.

Therefore, the objective of the present study was first to establish an extensive antigenic signature of NDEVs by testing a large panel of 54 antibody specificities known to be expressed on the PMN and selecting those generating the highest detection signal while preserving good specificity. Based on these new insights into the NDEVs surface profile, we next developed a new strategy to overcome the low fluorescence signal of NDEVs, combining a selection of the best antibody specificities used as a cocktail and a reduction of background noise by size-exclusion chromatography. Finally, the performance of this new strategy, with enhanced sensitivity, was used to improve NDEVs detection in plasma from sepsis patients and make the sorting of NDEVs from COVID-19 patients feasible.

2 | MATERIAL AND METHODS

2.1 | Sample processing

Blood samples used for EVs analysis or sorting were collected from sepsis, COVID-19 patients or healthy donors enroled in the study approved by the Medical Ethics Committee of Aix-Marseille University. Samples were collected and processed according to the International Society on Thrombosis and Hemostasis and International Society of Extracellular Vesicles (ISEV) guidelines (Coumans et al., 2017; Lacroix et al., 2012; Théry et al., 2018). Briefly, after a light tourniquet was applied, samples were drawn

from the antecubital vein using a butterfly device with a 21-gauge needle. Blood was collected into 2.7-ml Vacutainer tubes containing 0.129-mol/L sodium citrate (BD Diagnostics, Franklin Lakes, NJ, USA), and the first few millilitres were discarded. The samples were centrifuged twice at 2500 g for 15 min at room temperature (RT) to obtain platelet-free plasma (PFP). The PFP was homogenized and stored at −80°C until use.

2.2 | Cell isolation

PMNs were collected from three independent healthy donors (Blood Bank, Etablissement Français du Sang, Marseille). Cells were isolated from whole blood collected on anticoagulant citrate dextrose. First, PMNs and mononuclear cells were separated using gradient density separation (1.077 g/ml, lymphocyte separation medium, Eurobio, Courtaboeuf, France) and centrifuged at 500 g for 20 min. The upper part of the gradient was discarded, and peripheral blood mononuclear cells (PBMCs) were collected independently from the neutrophil-red blood cell fraction. Red blood cells were lysed using 50-mM ammonium chloride buffer for 10 min. PMNs were washed with Ca/Mg-free phosphate-buffered saline (PBS), bovine serum albumin (BSA) 0.1%, centrifuged for 5 min at 300 g and resuspended in PBS and BSA 0.1% buffer. Second, PMNs were purified by immunomagnetic separation using anti-CD66bAPC (allophycocyanin) antibody staining and then anti-APC magnetic beads (Miltenyi Biotec, Bergisch Gladbach, Germany). For monocytes, PBMCs were stained with the same process but using an anti-CD14APC antibody. Cell separation was realized with an autoMACS Pro Separator (Miltenyi Biotec). All steps were performed at 4°C to avoid cell activation.

The main lymphocyte cell subsets were purified from PBMCs by FCM cell sorting using MoFlo Astrios EQ (Beckman Coulter, Villepinte, France), and the following staining strategy was used: anti-CD45ECD (R-phycoerythrin Texas Red-X) (J33), anti-CD3PB (Pacific Blue) (UCHT1), anti-CD4FITC (fluorescein isothiocyanate) (13B8.2), anti-CD8BV785 (Brillant Violet) (SK1, Biolegend, San Diego, California, USA), anti-CD56PC7 (Phycoerythrin Cyanin 7) (N901), anti-CD19APCAlexa700 (HIB19, Biolegend), anti-CD14PE (phycoerythrin) (RMO52) and anti-CD66bAPC (80H3). All antibodies except anti-CD8 and anti-CD19 were purchased from Beckman Coulter. A washing step (300 g, 5 min) was performed to remove unbound antibodies. Cells were gated in FSC/SSC, and the doublets were excluded using an FSC width–FSC height dot plot. Lymphocytes were selected with a CD45/SSC chart. TCD4, TCD8, B and NK cells were sorted according to their phenotype: CD3+/CD4+, CD3+/CD8+, CD19+/CD3− and CD56+/CD3−, respectively. Residual neutrophils and/or monocytes were removed using CD66b/CD14 dot plot exclusion. Fluorescence leakage was corrected using monostaining samples. Cell sorting was realized using a 70-μm nozzle with 60 psi pressure sheath fluid.

Cell purity checked by FCM was above 95% for each leukocyte subset. Leukocyte subsets were incubated at 5.10^5 cells/ml in 0.22-μm filtered Roswell Park Memorial Institute medium (RPMI) supplemented with 10% foetal bovine serum depleted from Annexin-stained EVs. When mentioned, PMNs were stimulated with N-formylmethionine-leucyl-phenylalanin (fMLP) at 2 μM. PMNs activation was confirmed by increased ICAM-1 expression (CD54PE, 84H10). The supernatant was collected 24 h after incubation.

2.3 | Extracellular vesicles isolation and purification

The culture medium supernatant was centrifuged twice for 5 min at 300 g to pellet cell and once at 2500 g for 10 min to remove apoptotic bodies. EVs were then concentrated by 100-kDa ultrafiltration at 1000 g for 15 min (UFC910008 Amicon Ultra15 Merck, Darmstadt, Germany) and purified from soluble proteins by size exclusion chromatography (SEC) on qEVoriginal/70-nm columns provided by Izon Science (Oxford, England). Purified EVs were concentrated again by ultrafiltration and stored at −80°C in PBS-/- aliquots at 1.10^3 EV/μL, after enumeration by FCM, using Annexin V positive staining, according to Cointe et al. (Cointe et al., 2017). We have submitted all relevant data of our experiments to the EV-TRACK knowledgebase (EV-TRACK ID: EV210214) (Van Deun et al., 2017).

3 | EVS FLOW CYTOMETRY ANALYSIS

3.1 | EVs gating strategy and staining protocol

A detailed protocol is provided in the supplemental file according to the MIFlowCyt-EV guidelines (Welsh et al., 2020). Briefly, EVs analysis by FCM was performed using a 4-laser (Violet–Blue–Yellow–Red) CytoFLEX S cytometer (Beckman Coulter) provided with a plate reader. Instrument performances were checked daily using CytoFLEX Daily QC fluorosphere beads and SPHERO Rainbow 8-peak (Spherotech, Lake Forest, USA). The stability of the large EVs scatter gate was monitored by the use of

Megamix-Plus Forward Scatter (FSC) and Side Scatter (SSC) purchased from BioCytex (Marseille, France). The gating strategy is illustrated in Supplemental Figure S1.

Regarding the staining step, all antibodies were centrifuged for 2 min at 13,000 g to remove aggregates prior to use. EVs (30 μL) were incubated with 10 μL of Annexin V-FITC (AnnV) (Beckman Coulter) and 10 μL of the antibody(ies) of interest (Ab). The best antibody concentration was determined after titration on NDEVs (Supplemental Figure S2). After 20 min of incubation at RT, samples were diluted in 150 μL of AnnV binding buffer and analysed. To prevent carryover issues, a washing well was performed between each sample. To validate the staining efficiency in a complex environment, NDEVs were spiked in large EV-free plasma generated by serial filtration at 0.22 μm. For some experiments, the unbound antibody was removed by an SEC column (Izon, Oxford, UK).

3.2 | Antibody specificities

CD10PE (ALB1), CD105PE (TEA3/17.1.1), CD106PE (1G11), CD109PE (8A3), CD116PE (SCO6), CD11aPE (25.3), CD11bPE (Bear1), CD11cPE (BU15), CD120bPE (80M2), CD122PC7 (CF1), CD123PE (SSDCLY107D2), CD126PE (M91), CD13PE (SJ1D1), CD14PE (RMO52), CD15PE (80H5), CD157PE (SY/11B5), CD16PE (3G8), CD166PE (3A6), CD18PE (7E4), CD184PE (12G5), CD24PE (ALB9), CD26PE (4EL-1C7), CD300aPE (E59.126), CD31PE (1F11), CD32PE (2E1), CD328PE (Z176), CD33PE (D3HL60.251), CD36APC (FA6.152), CD40PE (MAB89), CD43PE (DFT1), CD44PE (J.173), CD45PE (J33), CD48ECD (J4.57), CD49dAPC (HP2/1), CD54PE (84H10), CD55PE (JS11KSC2.3), CD58PE (AICD58), CD59PE (MEM-43), CD62LPE (DREG56), CD62P-PE (CLBThromb/6), CD64PE (22), CD65PB (88H7), CD66bAPC (80H3), CD66cPE (KOR-SA3544), CD69PE (TP1.55.3), CD85dPE (42D1), CD85jPE (HP-F1), CD85kPE (ZM3.8), CD86PE (HA5.2B7), CD90PE (F15-42-1-5), HLA-DR-PE (Immu-357), LactoferrinPE (CLB13.17), OSCAR-PE (11.1CN5), TIA-1PE (2G9A10F5) were provided by Beckman Coulter. CD66bPE (G10F5) was purchased from BioLegend.

3.3 | Positivity threshold definition

The positivity threshold was set up as follows: (1) the best concentration of the antibody of interest was determined using a 5-point titration curve of the antibody of interest on NDEVs. (2) The best-matched isotype concentration was determined performing a 11-point titration curve of the isotypic antibodies on AnnexinV-stained NDEVs. The best isotypic antibody concentration was chosen so that the PE median fluorescence intensity (MFI) was the closest between the background noise (AnnexinV negative events) of EV stained with the antibody of interest and EV stained with the isotypic antibody (Supplemental Figure S3A–D). It was also checked that the PE signal of the specific and isotype antibodies was equivalent in buffer without EV (Supplemental Figure S4). This strategy allows taking into account the potential difference not only of fluo/prot ratio but also of free PE between de two antibodies. (3) The positive threshold was defined as the 99th percentile of PE signal generated by the isotypic antibody (Supplemental Figure S3E–G).

3.4 | EVs sorting

Samples were sorted on an Astrios EQ (Beckman Coulter) provided with aerosol catcher and installed under a Class II PSM in a negative pressure L2 laboratory. A 70-μm nozzle was used, with 60 PSI sheath fluid pressure (drop frequency was approximately 95,000 Hz). The speed of sample acquisition was similar for all samples, with a limited number of events/s below 30,000 to sort with optimal conditions. PFP samples (100 μl) were stained with antibody(ies) at their optimal concentration and then diluted in binding buffer supplemented with hirudin (2 U/ml). For some conditions, SEC columns (qEV single 70-nm columns, Izon) were used prior to sorting to remove plasma soluble proteins and unbound antibody according to the manufacturer's instructions. The sorting strategy was first defined using Gigamix beads (mix vol:vol of Megamix+ FSC and SSC beads) to design a 0.16–0.9-μm bead-equivalent FSC gate. Fluorescence channels were set up and monitored with Sphero 8 peak beads to maintain fluorescence performance during the sorting experiments. Sorted NDEVs were defined as Annexin V-FITC/PE-conjugated antibody-positive/CD41-negative events and sorted platelet EVs were defined as Annexin V-FITC/CD41-APC-positive/PE-conjugated antibody-negative events.

3.5 | Transmission electron microscopy

Transmission electron microscopy was performed on pellets of NDEV obtained after SEC purification and ultracentrifugation at 100,000 g for 90 min. NDEV pellets were fixed in PFA 2% and glutaraldehyde 2.5% for 30 min at RT and stored in Hanks'

Balanced Salt Solution at 4°C. Then, NDEVs pellets were postfixed in 2% osmium for 1 h on ice, dehydrated in a gradient series of acetone baths and embedded in epoxy resin. Pellets were sectioned on a UC7 ultramicrotome (Leica, Wetzlar, Germany), and sections were contrasted with aqueous uranyl acetate 1% (10 min) and lead citrate (4 min). The grids were observed at 80 kV on an FEI Morgagni transmission electron microscope (Thermo Fisher, Waltham, USA), and images were acquired using a MegaView3 camera (Emsis, Muenster, Germany).

3.6 | Tunable resistive pulse sensing

Tunable resistive pulse sensing (TRPS) was performed using a qNano Gold TRPS measurement instrument (Izon, Oxford, UK). Before using the samples, the instrument was calibrated with CPC200 beads (mean diameter 210 nm). NP150 nanopore membranes stretched at approximately 41 nm were used. Voltage was set in 0.78V to achieve a stable current 110–1120 nA and pressure at 12 mbars, with root mean square noise below 10 pA. Samples and calibration beads were diluted in running buffer (PBS filtered under 0.22 μm). Samples were analysed using an NP150 nanopore (Izon). Measurement and analysis were performed with Izon Control Suite V3.3.3.2001 Software.

3.7 | Western blot

Western blot was performed on NDEV pellets obtained after SEC purification and ultracentrifugation at 100,000g for 90 min. NDEV pellets were lysed with RIPA buffer, next, separated on a 4%–12% NUPAGE gel under SDS or no-reducing conditions (for CD63) and then, transferred onto nitrocellulose membranes (Amersham Protran, Merck Sigma–Aldrich, St Quentin Fallavier, France). Membranes were blocked with 3% BSA/tris-buffered saline (TBS, ET220B, Euromedex, Souffelweyersheim, France) for 1 h at RT. Then, the membranes were incubated overnight at 4°C with antibodies against the designated antigens and purchased from Cell Signaling Technology, integrin β3 (1:1000, #4702), from Thermo Fisher Scientific CD63 (1:1000, #10628D), glyceraldehyde-3 phosphate dehydrogenase (GAPDH) (1:1000, #MAT-11114) and albumin (1:1000, #MA532531). Next, horseradish peroxidase (HRP)-conjugated secondary antibody (1:3000–1:5000, Pierce, Thermo Fisher) was added for 1 h at RT. Immunocomplexes were visualized by enhanced chemiluminescence (ECL or ECL femto) according to the manufacturer's instructions (Pierce, Rockford, IL, USA). Specific bands were detected using a G-BOX Imaging System (GeneSys, Cambridge, UK).

3.8 | Data analysis and statistic

All FCM data were analysed with Kaluza analysis 2.1 software. Data were analysed for their statistical relevance with GraphPad Prism 8 software (GraphPad Software). Statistical tests used were either Mann–Whitney or paired Student's *t* tests, depending on the experiment. The results are presented as the mean ± standard deviation, if not stated otherwise.

4 | RESULTS

4.1 | Characterization of NDEVs

According to the Minimal Information for Studies of Extracellular Vesicles 2018 (MISEV) (Théry et al., 2018), NDEVs were purified from PMN culture media (Figure 1A) and characterized as EVs structures using several methods. First, the presence of a bilayer phospholipid membrane-enclosed large EVs was demonstrated by transmission electronic microscopy (Figure 1B) and by a significant reduction in AnnexinV-stained EVs counts in FCM after Triton lysis and 0.1-μm filtration (Figure 1C). Second, the presence of typical membranous and cytosolic EV-associated molecules was shown by the fixation of AnnV on purified NDEVs using FCM (Figure 1C), and the presence of integrin subunit β3 and GAPDH was revealed by Western blot without major contamination by soluble molecules like albumin (Figure 1D). Finally, TRPS assays showed that the vesicles had a median size of 191 ± 105 nm (Figure 1E). Taken together, the structural, molecular and size features of NDEVs preparations were in accordance with the definition of EVs.

4.2 | Determination of a selective antigenic signature of NDEVs

Based on fifty-four antigenic specificities known to be expressed on leukocytes, a large phenotypic characterization of NDEVs was performed. Antibody labelling efficiency was defined by the percentage of AnnV-FITC+/antibody-PE+ NDEVs

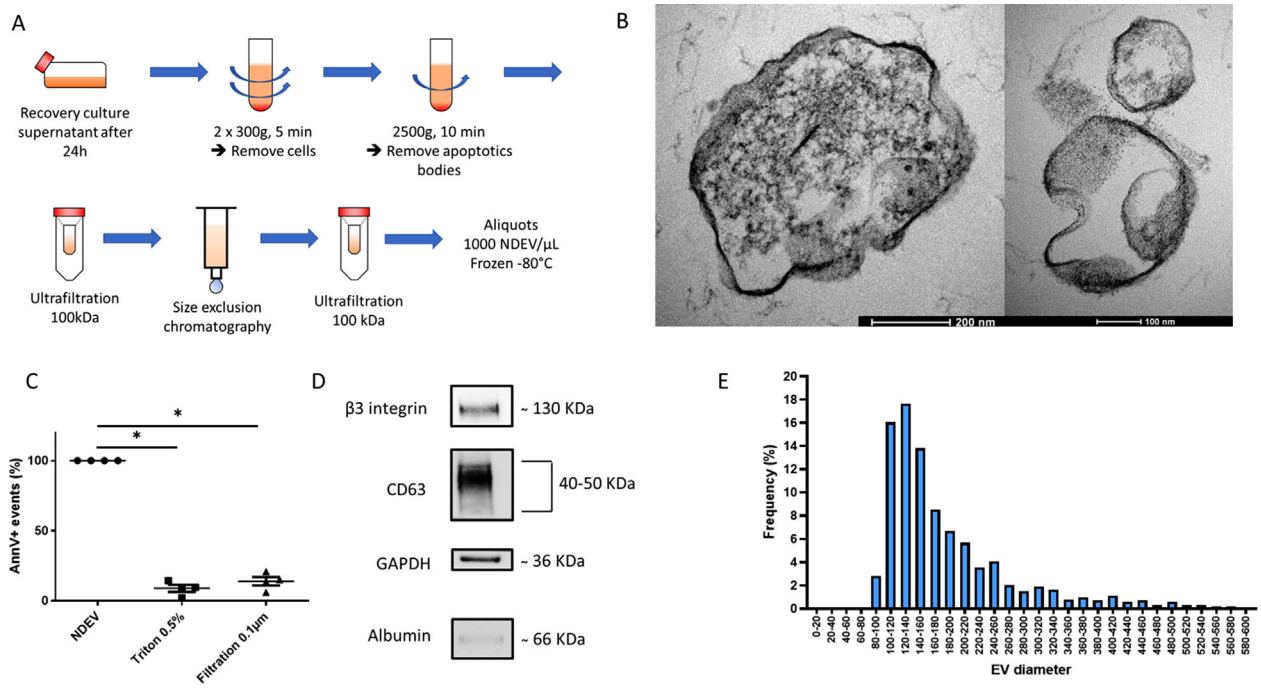

FIGURE 1 Production and characterization of neutrophil-derived extracellular vesicles (NDEVs). (A) Preparation and purification of NDEVs: NDEVs were collected from purified neutrophil supernatants (basal or stimulated cells). Then, they were purified by serial centrifugation (to remove dead cells and apoptotic bodies), ultrafiltration, size exclusion chromatography and a second ultrafiltration. Purified NDEVs were numerated to generate aliquots of 1000 NDEV/μl. (B) Images of NDEVs by transmission electron microscopy. (C) Effect of Triton 0.5X buffer and 0.1-μm filtration on NDEVs by flow cytometry. (D) Western blot (protein load in μg of NDEV). (E) Size distribution by tunable resistive pulse sensing (qNano) with p200 nanopores. GAPDH, glyceraldehyde-3 phosphate deshydrogenase

(double-positive NDEVs) among total AnnV+ NDEVs and displayed as a heat map, from 0% dark blue (no double-positive EVs) to 100% red, as shown in Table 1. According to their percentage of double-positive labelling, the positive markers were considered to be undetectable below 14% or positive at low (between 14% and 45%), medium (between 40% and 55%) or high (higher than 55%) expression AnnexinV-stained EVs.

Strikingly, among the 54 tested specificities, only 15 were classified as positive on NDEVs with a significant detection above a threshold of 14%. CD15, CD24 and CD18 were the markers with the highest expression. CD59, CD65, CD11b, CD66b, CD157 and CD66c displayed median expression, whereas CD45, CD16, lactoferrin, CD13, CD32 and TIA-1 were detectable at lower percentages. Similar results were obtained when the detection of spontaneously generated NDEVs was compared to fMLP-induced NDEVs, except for slightly higher expression of TIA-1 and lower expression of CD15, CD24, CD59 and CD157.

To assess the specificity of the positive markers at the EVs scale, the 15 positive antibodies were tested on EV derived from monocyte and lymphocyte subsets (TCD4, TCD8, B and NK). As expected, the panleukocyte marker CD45 was found to be expressed on all EV subsets (Table 2). Other antibodies with broad expression, such as CD18 or CD59, were also expressed on other leukocyte EV subpopulations, whereas others were detected on at least another one EV subpopulation of leukocyte origin: CD24 and CD65 (B cells), CD11b (monocytes and NK cells) and CD157 (monocytes). Finally, eight markers appeared to be selectively expressed by NDEVs: CD15, CD66b, CD66c, CD16, lactoferrin, CD13, CD32 and TIA-1. Among them, selecting markers generating the highest detection signal while preserving good specificity led us to choose CD15, CD66b and CD66c to define a selective antigenic signature defining NDEVs.

Next, to determine the staining robustness of these three antibodies in a more complex environment, NDEVs enumeration was performed on NDEV-spiked large EV-free plasma. As shown in Figure 2A, CD15, CD66c and CD66b labelling was detectable using NDEVs concentrations as low as 50 NDEVs/μL. Moreover, NDEVs detection remained linear ($r^2 > 0.98$) over the total range of concentrations from 50 to 800 NDEVs/μL (Figure 2B).

In summary, CD15, CD66c and CD66b specificities were therefore validated as the best candidates for defining a selective NDEVs antigenic signature reliable for their detection by FCM to selectively detect NDEVs in simple or complex biofluids.

4.3 | New strategy to improve the detection of NDEVs by flow cytometry

Having defined a selective antigenic signature of NDEVs, we therefore developed a new strategy to overcome their low fluorescent signal by reducing background noise and increasing the fluorescent signal.

TABLE 1 Extensive phenotyping of neutrophil-derived extracellular vesicles (NDEVs) from basal and stimulated cells

	NDEV						NDEV				
Stimuli	No		fMLP			Stimuli	No		fMLP		
	Mean	SD	Mean	SD	*p-value*		Mean	SD	Mean	SD	*p-value*
CD15	87,5	5,7	84,1	4,4	*0.057*	CD85d	2,2	0,8	2,2	0,7	*>0.999*
CD24	69,4	14,9	61,5	12,4	*0.115*	CD14	2,0	2,0	0,7	1,0	*0.453*
CD18	56,5	5,2	50,7	4,6	*0.194*	CD40	1,9	2,5	1,6	2,3	*0.356*
CD59	55,2	13,0	52,8	14,4	*0.146*	CD85j	1,7	2,5	1,1	1,5	*0.392*
CD65	51,4	25,8	50,1	23,8	*0.310*	CD11a	1,6	1,0	1,9	1,5	*0.528*
CD11b	48,7	19,8	42,2	16,6	*0.284*	CD120b	1,6	0,4	1,7	1,0	*0.912*
CD66b	43,8	12,8	49,8	1,3	*0.714*	CD300a	1,5	0,4	1,8	0,6	*0.149*
CD157	43,3	11,8	38,9	10,2	*0.126*	CD328	1,4	0,2	1,6	0,7	*0.560*
CD66c	41,2	13,8	42,8	11,3	*0.823*	CD86	1,1	0,7	0,9	1,0	*0.499*
CD45	39,2	12,0	35,2	8,2	*0.246*	CD26	1,0	1,3	0,8	1,0	*0.270*
CD16	34,4	12,9	25,9	5,2	*0.292*	CD184	1,0	0,9	1,1	1,1	*0.667*
Lactoferrin	25,6	5,3	26,6	4,1	*0.535*	CD126	0,7	1,0	0,4	0,6	*0.356*
CD13	19,9	8,1	16,9	6,2	*0.339*	CD109	0,7	0,6	0,4	0,5	*0.297*
CD32	19,9	6,2	17,2	2,4	*0.564*	CD64	0,6	0,5	0,5	0,4	*0.580*
TIA-1	14,7	0,6	24,6	2,6	*0.169*	OSCAR	0,5	0,3	0,7	0,2	*0.300*
CD31	13,5	2,2	13,6	2,3	*0.156*	CD166	0,5	0,5	0,5	0,3	*0.635*
CD55	12,1	1,7	9,9	1,0	*0.057*	CD62L	0,5	0,3	0,3	0,0	*0.444*
CD10	11,0	2,9	11,8	1,3	*0.765*	CD123	0,5	0,6	0,5	0,5	*>0.999*
CD44	9,5	1,4	9,5	2,7	*0.807*	CD116	0,4	0,6	0,5	0,6	*0.423*
CD43	9,1	1,1	8,8	1,0	*0.732*	CD54	0,4	0,0	0,3	0,1	*0.225*
CD11c	6,4	1,4	5,7	0,7	*0.403*	CD90	0,4	0,5	0,4	0,7	*0.635*
CD69	5,7	2,5	10,0	10,2	*0.445*	CD105	0,3	0,1	0,2	0,2	*0.456*
CD49d	3,4	3,2	2,3	2,5	*0.110*	CD106	0,3	0,2	0,2	0,1	*0.808*
CD58	3,1	0,6	3,1	0,9	*0.935*	HLADR	0,3	0,5	0,3	0,5	*>0.999*
CD33	2,7	3,0	2,3	3,3	*0.473*	CD62P	0,2	0,4	0,3	0,5	*0.423*
CD36	2,6	3,3	2,4	3,5	*0.336*	CD122	0,2	0,2	0,2	0,2	*>0.999*
CD48	2,3	0,9	2,2	1,0	*0.754*	CD85k	0,2	0,2	0,2	0,3	*0.742*

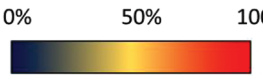

NDEVs were phenotyped with a panel of 54 selected markers. The heat map illustrates NDEVs detection from 0% (dark blue) to 100% (red) Annexin V-FITC+/PE+ EVs. The results were generated from three independent healthy donors. Data are presented as the mean value of triplicates with standard deviation (SD).
Abbreviation: fMLP, N-Formylmethionin-leucyl-phenylalanin.

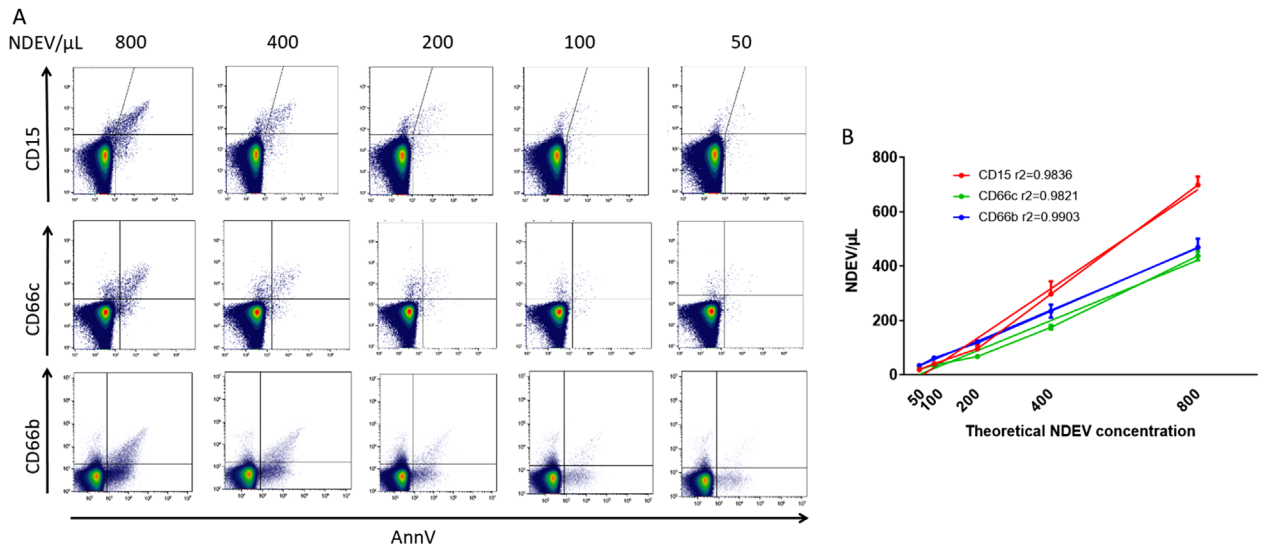

FIGURE 2 Linearity of neutrophil-derived extracellular vesicles (NDEVs) detection. (A) NDEVs were supplemented in large-extracellular vesicle (EV)-free plasma and stained with Annexin V FITC and PE antibodies. Three antibodies were tested on large EV-free plasma supplemented with NDEV: CD15, CD66b and CD66c. (B) NDEVs concentrations between 50 and 800 Annexin V + FITC NDEV/μL obtained by serial dilutions of NDEVs spiked-in plasma. A regression curve for each antibody was generated using three independent experiments. AnnV, AnnexinV

TABLE 2 Evaluation of specificity for the positive neutrophil-derived extracellular vesicles (NDEVs) markers

	EV derived from											
	Neutrophil		Monocyte		B cells		CD4+ T cells		CD8+ T cells		NK cells	
	Mean	SD	Mean	SD	Mean	SD	Mean	SD	Mean	SD	Mean	SD
CD15	87,5	5,7	4,5	2,5	5,5	0,2	7,2	2,5	8,4	1,0	4,8	0,7
CD24	69,4	14,9	3,5	1,5	22,9	7,6	8,1	3,7	7,1	5,6	5,0	1,9
CD18	56,5	5,2	46,8	10,0	6,9	1,7	30,8	15,1	39,1	23,4	39,6	10,9
CD59	55,2	13,0	8,3	0,2	13,9	5,2	42,0	10,8	27,4	6,8	18,7	7,4
CD65	51,4	25,8	8,0	3,3	14,1	2,7	0,6	0,1	8,0	4,5	12,4	9,5
CD11b	48,7	19,8	29,9	20,7	7,6	4,7	7,1	3,7	11,7	5,8	24,6	4,4
CD66b	43,8	12,8	4,9	2,5	1,8	1,7	2,1	2,4	2,4	1,8	1,4	0,9
CD157	43,3	11,8	46,0	4,2	4,5	2,6	6,0	1,4	3,7	2,0	5,1	2,6
CD66c	41,2	13,8	2,3	2,0	2,6	0,7	4,1	2,1	4,3	1,6	3,1	2,1
CD45	39,2	12,0	40,7	1,4	38,8	11,9	52,2	10,6	60,1	13,1	51,2	12,2
CD16	34,4	12,9	1,9	1,2	6,2	1,2	3,3	0,1	4,4	2,0	4,8	4,4
Lactoferrin	25,6	5,3	2,8	2,1	7,9	2,5	4,2	3,4	5,1	4,2	3,7	2,4
CD13	19,9	8,1	6,5	3,4	9,2	2,8	6,9	4,0	8,9	5,4	6,6	1,0
CD32	19,9	6,2	5,3	1,1	5,6	1,8	7,0	4,2	6,4	1,6	4,3	2,9
TIA-1	14,7	0,6	3,0	0,8	4,9	1,7	3,4	1,5	5,6	4,9	7,4	3,9

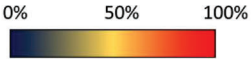

Antibodies that stained more than 14% of NDEVs were tested on EVs derived from other main leukocyte EVs subpopulations generated from resting cells: monocytes, CD4 T, CD8 T, B and NK cells. The heat map illustrates this detection from 0% (dark blue) to 100% (red) double-positive EVs. The results were generated from three independent healthy donors. Data are presented as the mean value of triplicates with standard deviation (SD).

The first objective of this strategy was to decrease the fluorescent background noise by removing the unbound antibody using SEC. To that aim, NDEVs were labelled with the three best markers (CD15, CD66b or CD66c) and the antibody specificities that allowed a detection higher than 40% of NDEVs. The staining was compared with or without SEC washing. As illustrated in Figure 3A, compared to the no-wash condition, the level of the background noise (grey dots) was reduced, and weakly stained NDEVs (blue dots) were detected after SEC. Combining all the specificities, including CD15, CD66b and CD66c, the MFI of the background noise was significantly reduced ($p = 0.03$) (Figure 2B), and the percentage of detected NDEVs was significantly increased ($p = 0.0051$) (Figure 3C) after washing with SEC.

Taken together, these results demonstrate that SEC improves the detection of NDEVs by reducing the fluorescent background noise.

The second objective of the new strategy was to increase the absolute fluorescent signal of NDEVs using the three selected antibodies (CD15, CD66b and CD66c) coupled with the same fluorochrome (PE) combined as a "cocktail". To that aim, NDEVs staining was compared after labelling with CD15 alone (best individual marker) versus different antibody mixes composed of two or three antibodies, with or without SEC washing. When the three-antibody cocktail was used without washing step by SEC, the MFI of NDEVs significantly increased compared to CD15, contrary to two-antibody cocktail (Figure 4A). However, the fluorescent background noise was also significantly increased (Figure 4B). Consequently, the separation index between NDEVs and background noise was not significantly improved (Figure 4C), and finally, the percentage of NDEVs detection was significantly decreased (CD15: 86% ± 3 vs. CD15/66b/66c: 80% ± 2, $p = 0.03$, Figure 4D). In contrast, when the three antibodies were used in combination, with a washing step by SEC, the MFI of NDEVs significantly increased compared to CD15 alone (Figure 4A), without an increase in the fluorescent background noise (Figure 4B). Consequently, the separation index between NDEVs and background noise was significantly increased (Figure 4C), and the percentage of detection of NDEVs was also significantly increased (CD15: 82% ± 3 vs. CD15/66b/66c: 91%% ± 4, $p = 0.008$, Figure 4D). This staining optimization was less efficient when combining only two antibodies for NDEVs labelling, resulting in a lower separation index and percentage of double-positive NDEVs.

Therefore, due to the observed synergy, a new strategy––combining a cocktail of the three selected antibodies CD15, CD66b and CD66c, in association with the washing step using SEC was proposed to improve NDEVs detection.

4.4 | Validation of the new combined strategy to detect NDEVs by FCM

The added value of this new combined strategy to enumerate and sort NDEVs was further validated in sepsis and COVID-19 patients, two infectious contexts associated with immune-thrombotic and inflammatory complications.

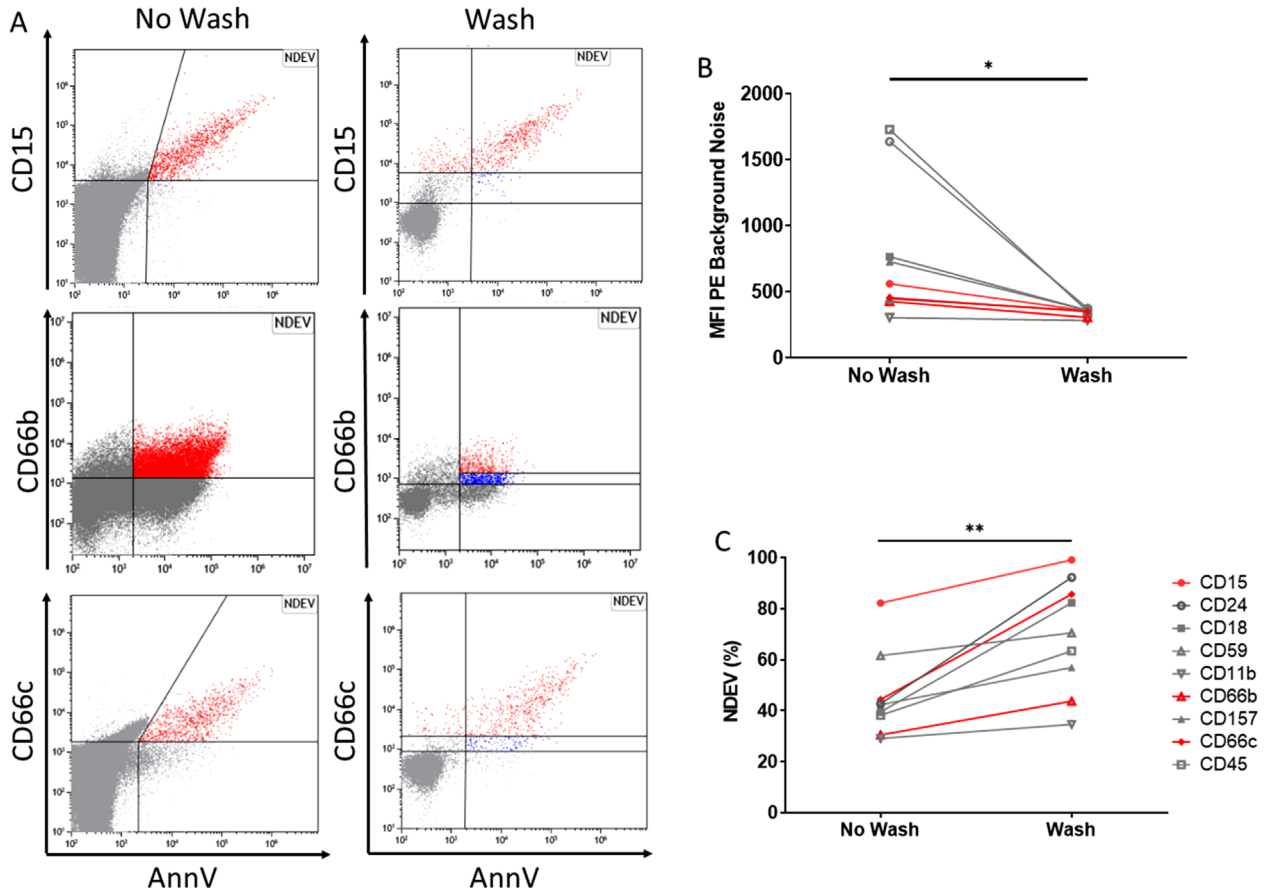

FIGURE 3 Impact of washing step (SEC) on neutrophil-derived extracellular vesicles (NDEVs) detection. (A) Representative graphs of CD15, CD66b and CD66c detection on extracellular vesicles (EVs) in no-wash (no SEC) and wash (SEC) conditions. Blue dots represent supplemental AnnV+/PE+ NDEVs detected in the wash protocol compared to red dots detected in both conditions. (B, C) PE median fluorescence intensity background noise (Annexin V FITC-/PE- events) and percentage of double-positive NDEVs detected among Annexin V+ FITC NDEVs between no wash and wash conditions for the nine antibodies tested. Ab, antibody; AnnV, Annexin V; SEC, size exclusion chromatography

The gain in sensitivity was first validated to improve NDEVs enumeration in sepsis patients by reference to a method using CD15 as a single labelling of NDEVs without a washing step. CD15 was chosen because extensive screening showed that it is the most detectable antibody specificity on NDEVs. Indeed, based on extensive screening, CD15 labelling was selected as those generating the highest detection signal while preserving good specificity. Under these conditions, an increase in AnnexinV-stained EVs of plasmatic NDEVs was detected when the new combined method was used, as illustrated in Figures 5A and 5B. This was confirmed in 10 sepsis patients, as shown by the significant increase in both the separation index (Figure 5C) and the concentration of NDEVs: 5120 ± 5070 and 16270 ± 13390 NDEVs/μL, respectively, for the current and the new combination strategy (Figure 5D).

Furthermore, to evaluate the impact of SEC washing on EVs detection, platelet-derived EVs were also measured with or without CD41-APC washing. The separation index and enumeration of platelet EVs were also significantly increased (Figures 5G and 5H, respectively).

Interestingly, the ratio between NDEVs and platelet EVs was significantly increased with the new combined method (Figure 5I, 0.3 ± 0.3 vs. 1.3 ± 1.4, $p = 0.002$). These data indicate that the enrichment of NDEVs in sepsis patients is due not only to the washing step but also to the combination of antibodies.

Additionally, because the sorting of EVs subpopulations can only be achieved if the fluorescence and/or light scattering signals of these subpopulations can be resolved, we investigated the benefit of the new combined method to sort NDEVs from the plasma of COVID-19 patients by comparison to a method using single labelling without a washing step by SEC. The sorting strategy, illustrated in Figure 6A, was defined first with the FSC scatter gate adjusted on 0.16- and 0.9-μm beads, then the selection of double-positive NDEVs (left panel) and finally, the exclusion of CD41-positive events from the NDEVs to sort (right panel). In the absence of the use of SEC for a washing step, sorting NDEVs using CD15 staining alone led to very limited NDEVs sorting mainly due to the high background noise. In contrast, using the SEC washing step, NDEVs sorting by CD15 was possible

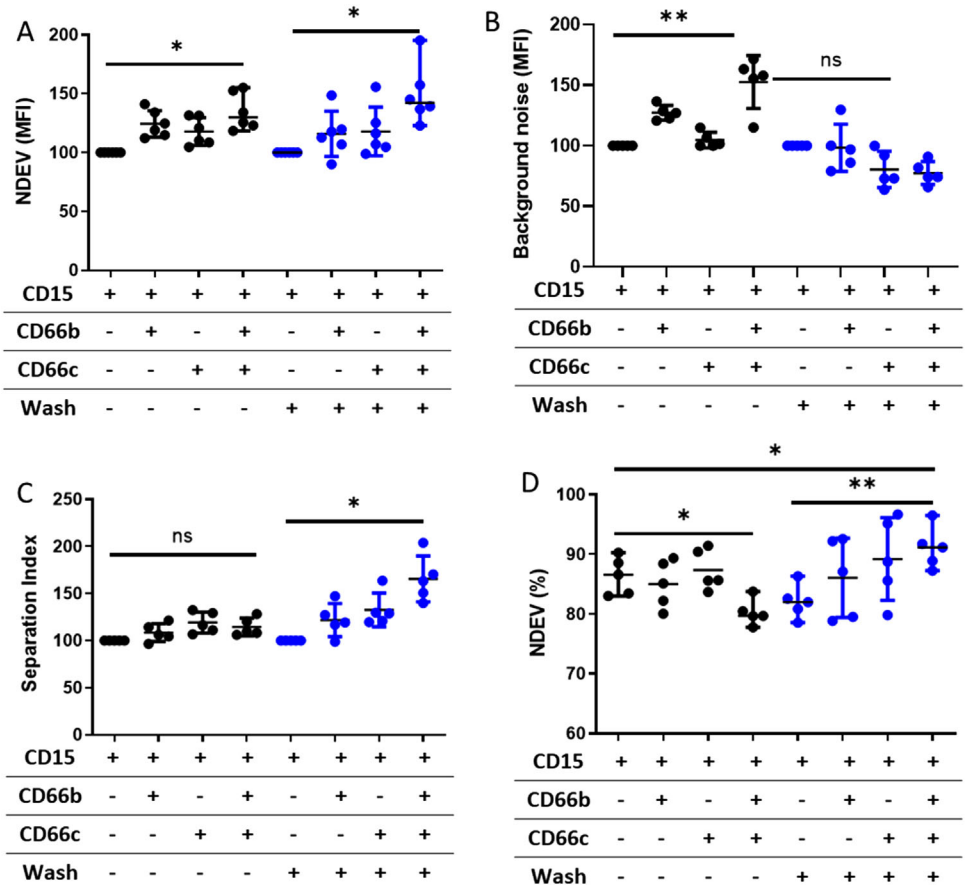

FIGURE 4 Impact of antibody combinations on neutrophil-derived extracellular vesicles (NDEVs) detection. The three best antibodies for the detection of NDEVs, CD15, CD66b and CD66b were associated at their optimal concentrations with the same PE fluorochrome in combination with AnnV FITC and were compared to CD15 staining alone. (A) PE median fluorescence intensity (MFI) of double-positive NDEV-detected, (B) PE MFI background noise, (C) separation index of NDEVs. SI was calculated using the formula: (PE MFI NDEV-PE MFI background noise)/2SD PE fluorescence background noise. (D) Percentage of double-positive NDEVs detected. This figure is the result of five independent experiments. MFI, median fluorescence intensity; SEC, size exclusion chromatography

(Figure 6B). Interestingly, in the new strategy, the added value of the three-antibody cocktail significantly increased the sorting of NDEVs compared to staining with CD15 alone.

Altogether, the new combined method made it feasible to efficiently sort NDEVs from COVID-19 patients.

5 | DISCUSSION

This work provides an extensive characterization of cell surface antigens conveyed by NDEVs, allowing us to identify a protein surface profile of 15 markers detectable by FCM, including four (CD157, CD24, CD65 and CD66c) never described on NDEVs. Using the screening assay results, CD15, CD66b and CD66c were identified as the best sensitive and specific markers to detect NDEVs and define a selective NDEVs antigenic signature reliable for their detection by FCM. Using this antigenic signature, to improve the detection of NDEVs by FCM, we propose a new strategy combining (1) labelling CD15, CD66b and CD66c antigens with a cocktail of three antibodies coupled with the same fluorochrome (PE) and (2) and washing-out unbound antibody by SEC. The increase in the fluorescent signal combined with the reduction in background noise allows a significant improvement in NDEVs counting in plasma from sepsis patients and makes efficient sorting of NDEVs from COVID-19 patients feasible.

FCM is currently used to detect NDEVs in the plasma of patients. However, this measurement remains challenging because of their small size and their low antigen density. Moreover, to date, the antibodies currently used for NDEVs detection have been selected empirically according to their antigenic expression on the parental cell. Surprisingly, among the 54 antigens already reported to be expressed on PMNs, only 15 were detectable on NDEVs. This may be due to the lack of exportation of some antigens on vesicle during the vesiculation process. Indeed, it is well known that some regions of the cellular membrane are more prone to vesiculate than others, such as lipid rafts (Skryabin et al., 2020; Salaün et al., 2004). Consequently, only a few

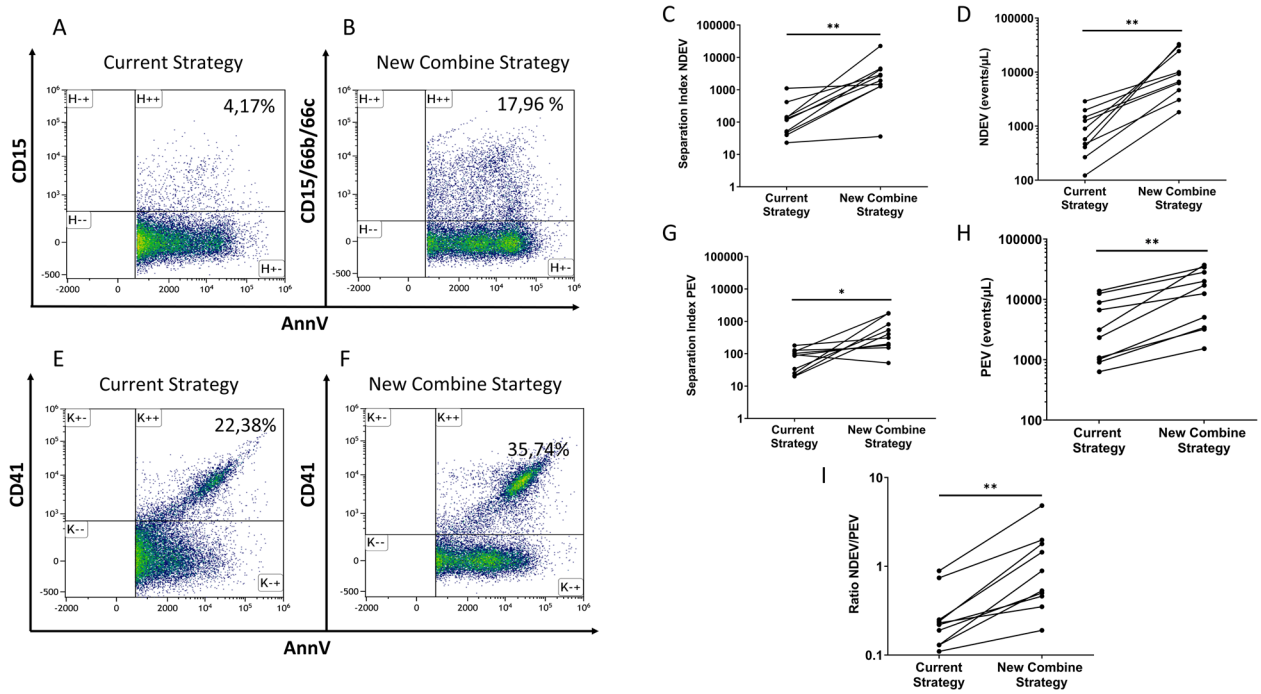

FIGURE 5 Neutrophil-derived extracellular vesicles (NDEVs) enumeration in sepsis patients. Ten platelet-free plasma samples from sepsis patients were stained according to the current or new combination strategy. For the current strategy, platelet-free plasma (PFP) was stained with AnnV-FITC, CD15-PE and CD41-APC without a washing step. New combination strategy: PFP stained with AnnV-FITC, CD15-PE, CD66b-PE, CD66c-PE and CD41-APC with a washing step. Representative graphs of Annexin V FITC+ NDEVs (A, B) and platelet EVs (E, F). The percentages indicated on the graph correspond to the proportion of NDEVs or platelet EVs among total AnnexinV-stained EV. (C, G) Comparison of the separation index for NDEVs and platelet EV, respectively. (D, H) NDEVs and platelet-EVs concentrations, respectively. (I) Ratio between platelet EVs and NDEVs quantification. AnnV, AnnexinV; PEV, platelet EVs

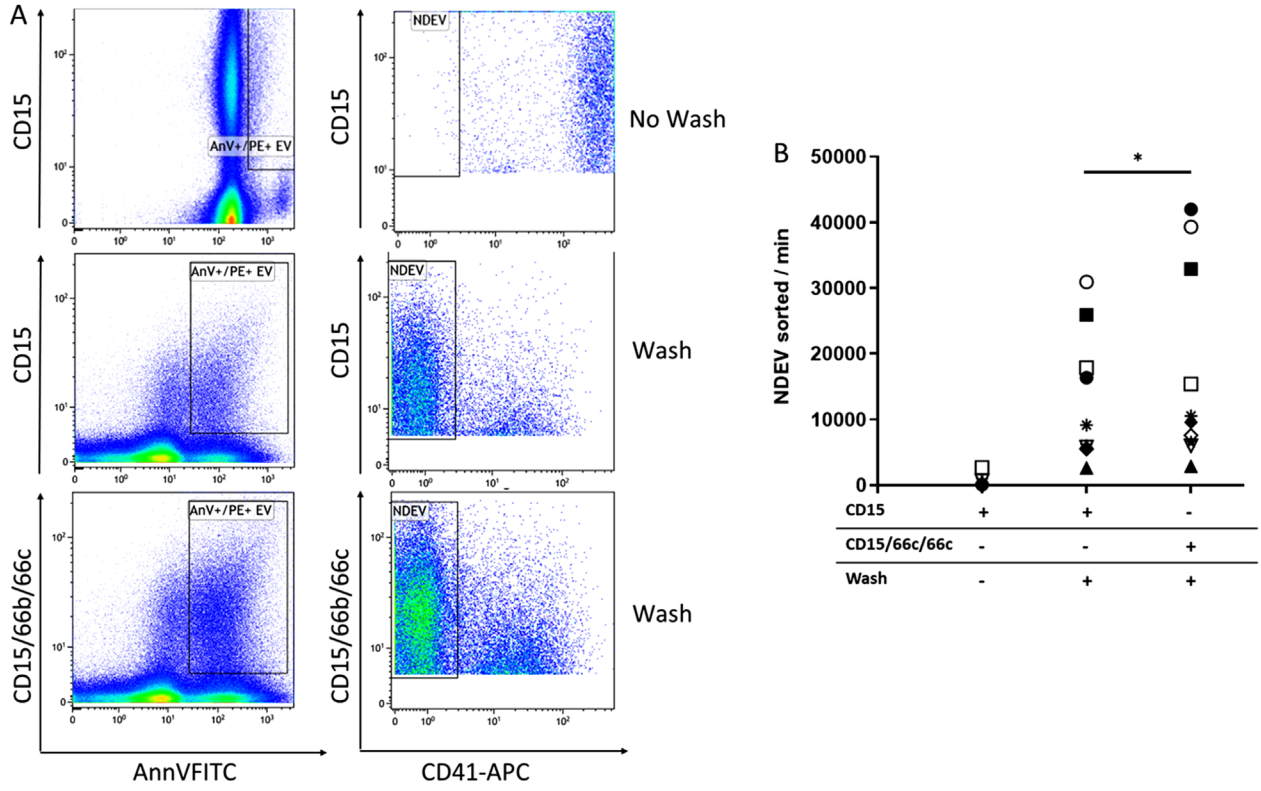

FIGURE 6 Neutrophil-derived extracellular vesicles (NDEVs) sorting in COVID-19 plasma. For each plasma sample, three pre-analytical conditions were tested: Annexin V FITC/CD15 PE staining without washing ($n = 5$), Annexin V FITC/CD15 PE staining, washing ($n = 10$), Annexin V FITC/CD15 CD66b CD66c PE staining ($n = 10$) and washing. For the three conditions, CD41 APCs were also added to the sample to exclude NDEVs CD41+ ($n = 5$). (A) Illustration of the dot plot showing NDEVs sorting by the three conditions. (B) Number of NDEVs sorted per minute

membrane proteins will be enriched on the EVs while others, although present at the cellular scale, are not detectable on the EVs generated (Jimenez et al., 2019; Jang et al., 2019). Although NDEVs detection was established using one of the most fluo-sensitive instruments available on the market (George et al., 2021), another explanation could be the expression of antigen with an insufficient density to be detectable by FCM. The limited detection of some antigens on NDEVs might also potentially be due to the epitopic specificity of the selected clone. However, the 54 clones used in this study were selected on the basis of positive expression on parental cells, suggesting distinct phenotypes between cells and EVs. In contrast, during the vesiculation process, it has been reported that some molecules, such as glycosylphosphatidylinositol (GPI)-anchored molecules were concentrated on EVs (Müller, 2018). Accordingly, among the 15 antigens detected in our work on NDEVs, six (40%) were GPI-anchored proteins (CD24, CD59, CD66b, CD157, CD66c and CD16). Identification of this molecular pattern provides not only chemical characteristics for selecting the best markers to quantify NDEVs in biological fluids but also information about NDEVs biological properties because some antigens, such as CD16 and CD32, are involved in immune regulation, whereas others, such as CD11b, CD18, CD15, CD24, CD66b, CD66c and CD157, are involved in cell adhesion, inflammation and migration.

Since antigenic density modulation on NDEVs may occur after stimuli-induced vesiculation, we investigated the effect of fMLP. Surprisingly, we found very little variation for the markers supposed to be affected by fMLP, in agreement with FCM-based results already reported for the lack of modulation of CD18 expression on EVs after exposure of PMN to fMLP (Gomez et al., 2020). The stability of the molecular antigen density at the EVs surface is clearly an advantage with regards to the selection of a generic marker useful to quantify NDEVs in various clinical settings; however, we cannot exclude that some inducers distinct from fMLP may more profoundly affect the antigenic phenotype conveyed by NDEVs.

In addition to the challenge of small size and low fluorescence inherent to all EVs and although no consensus exists on the normal value of EV subpopulations in healthy people, NDEVs belong to the "rare EV subsets" detectable in healthy people's plasma, such as leukocytes- or endothelial cells-derived EVs. Appropriately, one of the novelties of our FCM strategy was first to increase the fluorescent signal of NDEVs by associating three antibodies (CD15, CD66b and CD66c) conjugated with the same fluorochrome (PE). These three antibodies were selected because they generated the highest detection signal while preserving good specificity since they did not label EVs of monocytic nor lymphocytic (T, B and NK) origin. To our knowledge, such an association of three antibodies CD15n CD66b and CD66c cocktail to improve the detection of NDEVs has never been described yet.

However, the use of an antibody cocktail alone was not sufficient to improve the detection of NDEVs due to the increase in background noise generated by the accumulation of unbound antibodies or free fluorophores. To overcome this issue, we completed our strategy with a washing step by SEC to separate the labelled EVs from unbound antibodies and other contaminants. Indeed, several studies have previously shown that SEC was an efficient method to separate EVs from soluble proteins (Böing et al., 2014; Gámez-Valero et al., 2016; Gardiner et al., 2016; Mateescu et al., 2017) and to decrease fluorescence background noise on EVs with fluorescent dyes (Morales-Kastresana et al., 2017). The present study confirms that SEC improves EV-based biomarker detection using a cocktail antibody without increasing the associated background noise level. Nonetheless, the use of SEC can result in a loss of some AnnexinV-stained EVs, therefore making difficult the absolute numeration of EVs. A solution may consist of the addition of an internal standard. For example, labelled EVs at a known concentration could be included in all samples before the SEC process.

The new combined strategy allows us to improve the enumeration of NDEVs in plasma from patients with sepsis by reference to the currently used FCM protocol. In-depth analysis of the literature shows that CD66b is the most widely used marker for the measurement of NDEVs in clinical cohorts (Guimarães Júnior et al., 2019; Headland et al., 2015; Leroyer et al., 2007; Porro et al., 2010). In some cases, the strategy used for NDEVs detection was based on double labelling, for example, CD11b and CD18 (Herrmann et al., 2015) or CD66b and CD11b (O'dea et al., 2016). However, the present study shows that both CD11b and CD18 lack specificity for NDEVs, since CD11b was also detected on monocyte-derived EVs and CD18 on monocyte- and some lymphocyte-derived EVs. In addition to using diverse markers to detect NDEVs by FCM, such as CD15 or CD66b (Huisse et al., 2008; Nieuwland et al., 2000; Timár et al., 2013), almost every study used a different pre-analytic and labelling protocol, thus hindering comparison of results among studies. Consequently, a large range of values has been reported in the literature for the plasmatic level of NDEVs in healthy individuals (from undetectable to approximately 400 NDEVs per microliter). More importantly, the variability regarding pre-analytic and analytical protocols resulted in discrepancies regarding the main clinical message provided by NDEVs enumeration in a given clinical context. Regarding sepsis, most of the studies published in the literature agree in reporting increased NDEVs concentration when comparing sepsis or septic shock to healthy donors (Herrmann et al., 2015; Lehner et al., 2016; Lashin et al., 2018; O'dea et al., 2016), except for one of them (Mostefai et al., 2008). Nevertheless, there is no consensus about the relationship between this increase and patient survival. Some studies showed increased NDEV counts in nonsurviving patients (Chen et al., 2020; Danesh et al., 2018; Lehner et al., 2016), while others did not show such a correlation with death (O'dea et al., 2016; Mostefai et al., 2008). Interestingly, one study showed that increased levels of NDEVs coexpressing CD66b and α2-macroglobulin were associated with patient survival during sepsis (Lashin et al., 2018). In bronchoalveolar lavages from patients with acute respiratory distress syndrome, NDEVs were the only subset associated with a better outcome (Guervilly et al., 2011). However, other studies showed that increased NDEVs concentrations in plasma were also correlated with the occurrence of disseminated intravascular coagulation during sepsis (Stiel et al., 2016). In the above-cited

context of potential clinical interest, a robust strategy of NDEVs counting using FCM is mandatory to delineate their relevance as a pertinent biomarker.

The new combination strategy not only improves the detection of NDEV-based biomarkers but also makes efficient sorting of NDEVs feasible. In fact, compared to FCM-based detection, EVs sorting is currently very challenging because of several additional limits specific to cell sorting (Kormelink et al., 2016). Among them, sorting time, dilution and the limited purity of the sorted EVs tend to consider EVs sorting as an impractical solution for downstream applications, such as functional tests (Morales-Kastresana et al., 2019; Morales-Kastresana et al., 2020) or the analysis of their composition. Since the sorting of particles appears to be a fine compromise between purity, sensitivity and throughput, few studies have shown that the sorting of EVs is possible from cell culture supernatant. In particular, EVs from cancer cell lines and dendritic cells were sorted after labelling with only a cell tracker (Morales-Kastresana et al., 2019). However, to our knowledge, the sorting of EVs from plasmatic samples (Morales-Kastresana et al., 2019) has never been described. Our strategy that combines (i) enhanced sensitivity due to antibody combination and (ii) reduced background noise obtained by a post-labelling SEC washing step allows an efficient EVs sorting from plasma of COVID-19 patients. Because sorting offers the opportunity to study the content or functional activity of EVs with specific antigen expression, this opens the door to a better characterization of the biological role of NDEVs in COVID-19. Indeed, neutrophils play a role in COVID-19. Consequently, pathologies involving neutrophils and their derived products, such as neutrophil-extracellular traps (Leppkes et al., 2020; Tomar et al., 2020; Wang et al., 2020; Zuo et al., 2021) and NDEVs may well be also involved in COVID-19 pathophysiology (Guervilly et al., 2021; Krishnamachary et al., 2021). However, despite the improvement provided by our new strategy, some limitations remain, due to the limited initial volume of samples. It seems difficult to sort enough plasma EVs to perform assays such as proteomic or lipidomic that need high amount of EV. But it is conceivable to perform tests needing low amount of EVs, such as functional assays, FCM characterization or size determination by TRPS. For example, using the sorted NDEVs, we were able to measure a NDEV elastase activity (data not shown).

In conclusion, combining optimization led us to improved detection of NDEVs and enabled selective EVs sorting. This study opens new directions (1) to better understand the role of NDEVs in infectious diseases associated with immunothrombotic complications, (2) to provide a more reliable access to NDEVs by FCM. This may help future routine hospital use since this technique is present in many medical biology laboratories. Although the present study shows an improvement of NDEV detection by FCM in sepsis plasma samples, it is now warranted to test this new combined strategy on a more extensive clinical cohort of septic shock patients and on patients with other immunothrombotic and inflammatory disorders such as atherosclerotic and renal disorders (Daniel et al., 2006; He et al., 2016) or (ANCA)-associated vasculitis (Kambas et al., 2014). However, to make feasible the analysis of a large number of plasma samples, it could be necessary to use more adequate tools to process SEC after labelling. To overcome this limitation, more recent tools have been developed such as 96 well-plate SEC to purify EVs from biological samples. This strategy should also be applied to improve the FCM detection of other rare subpopulations of EVs generated by tissues with limited access, such as vascular endothelium, solid tumours or placenta.

ACKNOWLEDGMENT

We are grateful to Dr Emmanuel Gautherot and Dr Philippe Poncelet for their valuable scientific advice. We acknowledge Beckman Coulter, who provided reagents for this study.

AUTHOR CONTRIBUTIONS

Formal analysis: Amandine Bonifay, Stéphane Robert and Belinda Champagne. *Writing—original draft*: Amandine Bonifay and Stéphane Robert. *Writing—review and editing*: Amandine Bonifay, Stéphane Robert and Romaric Lacroix. *Data curation*: Loris Vallier, Corinne Chareyre, Paul-Rémi Petit and Aude Eugène. *Resources*: Mélanie Vélier and Shirley Fritz. *Conceptualization*: Amandine Bonifay, Stéphane Robert and Romaric Lacroix and Françoise Dignat-George. *Supervision*: Romaric Lacroix and Françoise Dignat-George.

REFERENCES

Böing, A. N., van der Pol, E., Grootemaat, A. E., Coumans, F. A. W., Sturk, A., & Nieuwland, R. (2014). Single-step isolation of extracellular vesicles by size-exclusion chromatography. *Journal of Extracellular Vesicles*, *3*. https://doi.org/10.3402/jev.v3.23430

Chen, H.-P., Wang, X.-Y., Pan, X.-Y., Hu, W.-W., Cai, S.-T., Joshi, K., Deng, L.-H., & Ma, D. (2020). Circulating neutrophil-derived microparticles associated with the prognosis of patients with sepsis. *Journal of Inflammation Research*, *13*, 1113–1124. https://doi.org/10.2147/JIR.S287256

Choi, D. S., Kim, D. K., Kim, Y. K., & Gho, Y. S. (2013). Proteomics, transcriptomics and lipidomics of exosomes and ectosomes. *Proteomics*, *13*(10–11), 1554–1571. https://doi.org/10.1002/pmic.201200329

Cointe, S., Judicone, C., Robert, S., Mooberry, M. J., Poncelet, P., Wauben, M., Nieuwland, R., Key, N. S., Dignat-George, F., & Lacroix, R. (2017). Standardization of microparticle enumeration across different flow cytometry platforms: Results of a multicenter collaborative workshop. *Journal of Thrombosis and Haemostasis*, *15*(1), 187–193. https://doi.org/10.1111/jth.13514

Connor, D. E., Exner, T., Ma, D. D. F., & Joseph, J. E. (2010). The majority of circulating platelet-derived microparticles fail to bind annexin V, lack phospholipid-dependent procoagulant activity and demonstrate greater expression of glycoprotein Ib. *Thrombosis and Haemostasis*, *103*(5), 1044–1052. https://doi.org/10.1160/TH09-09-0644

Cortez-Espinosa, N., Perez-Campos Mayoral, L., Perez-Campos, E., Alejandro Cabrera Fuentes, H., Perez-Campos Mayoral, E., Martínez-Cruz, R., Pina Canseco, S., Mayoral Andrade, G., Martinez Cruz, M., Gallegos Velasco, I., & Hernandez Cruz, P. (2017). Platelets and platelet-derived microvesicles as immune effectors in type 2 diabetes. *Current Vascular Pharmacology*, *15*(3), 207–217. https://doi.org/10.2174/1570161115666170126130309

Coumans, F. A. W., Brisson, A. R., Buzas, E. I., Dignat-George, F., Drees, E. E. E., El-Andaloussi, S., Emanueli, C., Gasecka, A., Hendrix, A., Hill, A. F., Lacroix, R., Lee, Y., Van Leeuwen, T. G., Mackman, N., Mäger, I., Nolan, J. P., Van Der Pol, E., Pegtel, D. M., Sahoo, S., … Nieuwland, R. (2017). Methodological guidelines to study extracellular vesicles. *Circulation Research*, *120*(10), 1632–1648. https://doi.org/10.1161/CIRCRESAHA.117.309417

Danesh, A., Inglis, H. C., Abdel-Mohsen, M., Deng, X., Adelman, A., Schechtman, K. B., Heitman, J. W., Vilardi, R., Shah, A., Keating, S. M., Cohen, M. J., Jacobs, E. S., Pillai, S. K., Lacroix, J., Spinella, P. C., & Norris, P. J. (2018). Granulocyte-derived extracellular vesicles activate monocytes and are associated with mortality in intensive care unit patients. *Frontiers in Immunology*, *9*, 956. https://doi.org/10.3389/fimmu.2018.00956

Daniel, L., Fakhouri, F., Joly, D., Mouthon, L., Nusbaum, P., Grunfeld, J.-P., Schifferli, J., Guillevin, L., Lesavre, P., & Halbwachs-Mecarelli, L. (2006). Increase of circulating neutrophil and platelet microparticles during acute vasculitis and hemodialysis. *Kidney International*, *69*(8), 1416–1423. https://doi.org/10.1038/sj.ki.5000306

Del Conde, I., Shrimpton, C. N., Thiagarajan, P., & López, J. A. (2005). Tissue-factor-bearing microvesicles arise from lipid rafts and fuse with activated platelets to initiate coagulation. *Blood*, *106*(5), 1604–1611. https://doi.org/10.1182/blood-2004-03-1095

Galdiero, M. R., Varricchi, G., Loffredo, S., Mantovani, A., & Marone, G. (2018). Roles of neutrophils in cancer growth and progression. *Journal of Leukocyte Biology*, *103*(3), 457–464. https://doi.org/10.1002/JLB.3MR0717-292R

Gámez-Valero, A., Monguió-Tortajada, M., Carreras-Planella, L., Franquesa M, la, Beyer, K., & Borràs, F. E. (2016). Size-exclusion chromatography-based isolation minimally alters extracellular vesicles' characteristics compared to precipitating agents. *Science Reports*, *6*, 33641. https://doi.org/10.1038/srep33641

Gardiner, C., Di Vizio, D., Sahoo, S., Théry, C., Witwer, K. W., Wauben, M., & Hill, A. F. (2016). Techniques used for the isolation and characterization of extracellular vesicles: results of a worldwide survey. *Journal of Extracellular Vesicles*, *5*, 32945. https://doi.org/10.3402/jev.v5.32945

Gaul, D. S., Stein, S., & Matter, C. M. (2017). Neutrophils in cardiovascular disease. *European Heart Journal*, *38*(22), 1702–1704. https://doi.org/10.1093/eurheartj/ehx244

George, S. K., Lauková, L., Weiss, R., Semak, V., Fendl, B., Weiss, V. U., Steinberger, S., Allmaier, G., Tripisciano, C., & Weber, V. (2021). Comparative analysis of platelet-derived extracellular vesicles using flow cytometry and nanoparticle tracking analysis. *International Journal of Molecular Sciences*, *22*(8), 3839. https://doi.org/10.3390/ijms22083839

Gomez, I., Ward, B., Souilhol, C., Recarti, C., Ariaans, M., Johnston, J., Burnett, A., Mahmoud, M., Luong, L. A., West, L., Long, M., Parry, S., Woods, R., Hulston, C., Benedikter, B., Niespolo, C., Bazaz, R., Francis, S., Kiss-Toth, E., … Ridger, V. (2020). Neutrophil microvesicles drive atherosclerosis by delivering miR-155 to atheroprone endothelium. *Nature Communication*, *11*(1), 214. https://doi.org/10.1038/s41467-019-14043-y

Guervilly, C., Bonifay, A., Burtey, S., Sabatier, F., Cauchois, R., Abdili, E., Arnaud, L., Lano, G., Pietri, L., Robert, T., Velier, M., Papazian, L., Albanese, J., Kaplanski, G., Dignat-George, F., & Lacroix, R. (2021). Dissemination of extreme levels of extracellular vesicles: Tissue factor activity in patients with severe COVID-19. *Blood Advances*, *5*(3), 628–634. https://doi.org/10.1182/bloodadvances.2020003308

Guervilly, C., Lacroix, R., Forel, J.-M., Roch, A., Camoin-Jau, L., Papazian, L., & Dignat-George, F. (2011). High levels of circulating leukocyte microparticles are associated with better outcome in acute respiratory distress syndrome. *Critical Care (London, England)*, *15*(1), R31. https://doi.org/10.1186/cc9978

Guimarães Júnior, M. H., Ferrari, T. C. A., Teixeira-Carvalho, A., Moreira, M. D. L., De Souza Santos, L. J., Costa-Silva, M. F., Coelho, R. M. P., Pinto, P. H. O. M., Ris, T. H., Salles, J. T., Passos, L. S. A., & Nunes, M. C. P. (2019). Cell-derived microvesicles in infective endocarditis: Role in diagnosis and potential for risk stratification at hospital admission. *Journal of Infection*, *79*(2), 101–107. https://doi.org/10.1016/j.jinf.2019.06.005

He, Z., Zhang, Y., Cao, M., Ma, R., Meng, H., Yao, Z., Zhao, L., Liu, Y., Wu, X., Deng, R., Dong, Z., Bi, Y., Kou, J., Novakovic, V., Shi, J., & Hao, L. (2016). Increased phosphatidylserine-exposing microparticles and their originating cells are associated with the coagulation process in patients with IgA nephropathy. *Nephrology, Dialysis, Transplantation*, *31*(5), 747–759. https://doi.org/10.1093/ndt/gfv403

Headland, S. E., Jones, H. R., Norling, L. V., Kim, A., Souza, P. R., Corsiero, E., Gil, C. D., Nerviani, A., Dell'accio, F., Pitzalis, C., Oliani, S. M., Jan, L. Y., & Perretti, M. (2015). Neutrophil-derived microvesicles enter cartilage and protect the joint in inflammatory arthritis. *Science Translational Medicine*, *7*(315), 315ra190. https://doi.org/10.1126/scitranslmed.aac5608

Herrmann, I. K., Bertazzo, S., O'callaghan, D. J. P., Schlegel, A. A., Kallepitis, C., Antcliffe, D. B., Gordon, A. C., & Stevens, M. M. (2015). Differentiating sepsis from non-infectious systemic inflammation based on microvesicle-bacteria aggregation. *Nanoscale*, *7*(32), 13511–13520. https://doi.org/10.1039/C5NR01851J

Hong, C. W. (2018). Extracellular vesicles of neutrophils. *Immune Network*, *18*(6), e43. https://doi.org/10.4110/in.2018.18.e43

Huisse, M.-G., Pease, S., Hurtado-Nedelec, M., Arnaud, B., Malaquin, C., Wolff, M., Gougerot-Pocidalo, M.-A., Kermarrec, N., Bezeaud, A., Guillin, M.-C., Paoletti, X., & Chollet-Martin, S. (2008). Leukocyte activation: the link between inflammation and coagulation during heatstroke. A study of patients during the 2003 heat wave in Paris. *Critical Care Medicine*, *36*(8), 2288–2295. https://doi.org/10.1097/ccm.0b013e318180dd43

Jang, S. C., Crescitelli, R., Cvjetkovic, A., Belgrano, V., Olofsson Bagge, R., Sundfeldt, K., Ochiya, T., Kalluri, R., & Lötvall, J. (2019). Mitochondrial protein enriched extracellular vesicles discovered in human melanoma tissues can be detected in patient plasma. *Journal of Extracellular Vesicles*, *8*(1), 1635420. https://doi.org/10.1080/20013078.2019.1635420

Jimenez, L., Yu, H., McKenzie, A. J., Franklin, J. L., Patton, J. G., Liu, Q., & Weaver, A. M. (2019). Quantitative proteomic analysis of small and large extracellular vesicles (EVs) reveals enrichment of adhesion proteins in small EVs. *Journal of Proteome Research*, *18*(3), 947–959. https://doi.org/10.1021/acs.jproteome.8b00647

Kambas, K., Chrysanthopoulou, A., Vassilopoulos, D., Apostolidou, E., Skendros, P., Girod, A., Arelaki, S., Froudarakis, M., Nakopoulou, L., Giatromanolaki, A., Sidiropoulos, P., Koffa, M., Boumpas, D. T., Ritis, K., & Mitroulis, I. (2014). Tissue factor expression in neutrophil extracellular traps and neutrophil derived microparticles in antineutrophil cytoplasmic antibody associated vasculitis may promote thromboinflammation and the thrombophilic state associated with the disease. *Annals of the Rheumatic Diseases*, *73*(10), 1854–1863. https://doi.org/10.1136/annrheumdis-2013-203430

Kapoor, S., Opneja, A., & Nayak, L. (2018). The role of neutrophils in thrombosis. *Thrombosis Research*, *170*, 87–96. https://doi.org/10.1016/j.thromres.2018.08.005

Kolaczkowska, E., & Kubes, P. (2013). Neutrophil recruitment and function in health and inflammation. *Nature Reviews Immunology*, *13*(3), 159–175. https://doi.org/10.1038/nri3399

Kormelink, T. G., Arkesteijn, G. J. A., Nauwelaers, F. A., van den Engh, G., Nolte-'t Hoen, E. N. M., & Wauben, M. H. M. (2016). Prerequisites for the analysis and sorting of extracellular vesicle subpopulations by high-resolution flow cytometry. *Cytometry Part A*, *89*(2), 135–147. https://doi.org/10.1002/cyto.a.22644

Krishnamachary, B., Cook, C., Kumar, A., Spikes, L., Chalise, P., & Dhillon, N. K. (2021). Extracellular vesicle-mediated endothelial apoptosis and EV-associated proteins correlate with COVID-19 disease severity. *Journal of Extracellular Vesicles*, *10*(9), e12117. https://doi.org/10.1002/jev2.12117

Lacroix, R., Judicone, C., Poncelet, P., Robert, S., Arnaud, L., Sampol, J., & Dignat-George, F. (2012). Impact of pre-analytical parameters on the measurement of circulating microparticles: Towards standardization of protocol. *Journal of Thrombosis and Haemostasis*, *10*(3), 437–446. https://doi.org/10.1111/j.1538-7836.2011.04610.x

Lashin, H. M. S., Nadkarni, S., Oggero, S., Jones, H. R., Knight, J. C., Hinds, C. J., & Perretti, M. (2018). Microvesicle subsets in sepsis due to community acquired pneumonia compared to faecal peritonitis. *Shock (Augusta, Ga.)*, *49*(4), 393–401. https://doi.org/10.1097/SHK.0000000000000989

Lehner, G. F., Harler, U., Haller, V. M., Feistritzer, C., Hasslacher, J., Dunzendorfer, S., Bellmann, R., & Joannidis, M. (2016). Characterization of microvesicles in septic shock using high-sensitivity flow cytometry. *Shock (Augusta, Ga.)*, *46*(4), 373–381. https://doi.org/10.1097/SHK.0000000000000657

Leppkes, M., Knopf, J., Naschberger, E., Lindemann, A., Singh, J., Herrmann, I., Stürzl, M., Staats, L., Mahajan, A., Schauer, C., Kremer, A. N., Völkl, S., Amann, K., Evert, K., Falkeis, C., Wehrfritz, A., Rieker, R. J., Hartmann, A., Kremer, A. E., … Herrmann, M. (2020). Vascular occlusion by neutrophil extracellular traps in COVID-19. *EBioMedicine*, *58*, 102925. https://doi.org/10.1016/j.ebiom.2020.102925

Leroyer, A. S., Isobe, H., Lesèche, G., Castier, Y., Wassef, M., Mallat, Z., Binder, B. R., Tedgui, A., & Boulanger, C. M. (2007). Cellular origins and thrombogenic activity of microparticles isolated from human atherosclerotic plaques. *Journal of the American College of Cardiology*, *49*(7), 772–777. https://doi.org/10.1016/j.jacc.2006.10.053

Martínez, G. J., Barraclough, J. Y., Nakhla, S., Kienzle, V., Robertson, S., Mallat, Z., Celermajer, D. S., & Patel, S. (2017). Neutrophil-derived microparticles are released into the coronary circulation following percutaneous coronary intervention in acute coronary syndrome patients. *Bioscience Reports*, *37*(1). https://doi.org/10.1042/BSR20160430

Mateescu, B., Kowal, E. J. K., Van Balkom, B. W. M., Bartel, S., Bhattacharyya, S. N., Buzás, E. I., Buck, A. H., De Candia, P., Chow, F. W. N., Das, S., Driedonks, T. A. P., Fernández-Messina, L., Haderk, F., Hill, A. F., Jones, J. C., Van Keuren-Jensen, K. R., Lai, C. P., Lässer, C., Di Liegro, I., & Nolte-'T Hoen, E. N. M. (2017). Obstacles and opportunities in the functional analysis of extracellular vesicle RNA––an ISEV position paper. *Journal of Extracellular Vesicles*, *6*(1), 1286095. https://doi.org/10.1080/20013078.2017.1286095

Morales-Kastresana, A., Musich, T. A., Welsh, J. A., Telford, W., Demberg, T., Wood, J. C. S., Bigos, M., Ross, C. D., Kachynski, A., Dean, A., Felton, E. J., Van Dyke, J., Tigges, J., Toxavidis, V., Parks, D. R., Overton, W. R., Kesarwala, A. H., Freeman, G. J., Rosner, A., … Jones, J. C. (2019). High-fidelity detection and sorting of nanoscale vesicles in viral disease and cancer. *Journal of Extracellular Vesicles*, *8*(1), 1597603. https://doi.org/10.1080/20013078.2019.1597603

Morales-Kastresana, A., Musich, T. A., Welsh, J. A., Telford, W., Demberg, T., Wood, J. C. S., Bigos, M., Ross, C. D., Kachynski, A., Dean, A., Felton, E. J., Van Dyke, J., Tigges, J., Toxavidis, V., Parks, D. R., Overton, W. R., Kesarwala, A. H., Freeman, G. J., Rosner, A., … Jones, J. C. (2019). High-fidelity detection and sorting of nanoscale vesicles in viral disease and cancer. *Journal of Extracellular Vesicles*, *8*(1), 1597603.

Morales-Kastresana, A., Telford, B., Musich, T. A., Mckinnon, K., Clayborne, C., Braig, Z., Rosner, A., Demberg, T., Watson, D. C., Karpova, T. S., Freeman, G. J., Dekruyff, R. H., Pavlakis, G. N., Terabe, M., Robert-Guroff, M., Berzofsky, J. A., & Jones, J. C. (2017). Labeling extracellular vesicles for nanoscale flow cytometry. *Science Reports*, *7*(1), 1878. https://doi.org/10.1038/s41598-017-01731-2

Morales-Kastresana, A., Welsh, J. A., & Jones, J. C. (2020). Detection and sorting of extracellular vesicles and viruses using nanoFACS. *Current Protocols in Cytometry*, *95*(1), e81.

Mostefai, H. A., Meziani, F., Mastronardi, M. L., Agouni, A., Heymes, C., Sargentini, C., Asfar, P., Martinez, M. C., & Andriantsitohaina, R. (2008). Circulating microparticles from patients with septic shock exert protective role in vascular function. *American Journal of Respiratory and Critical Care Medicine*, *178*(11), 1148–1155. https://doi.org/10.1164/rccm.200712-1835OC

Müller, G. A. (2018). The release of glycosylphosphatidylinositol-anchored proteins from the cell surface. *Archives of Biochemistry and Biophysics*, *656*, 1–18. https://doi.org/10.1016/j.abb.2018.08.009

Nieuwland, R., Berckmans, R.ené J., Mcgregor, S., BöIng, A. N., Th. Romijn, M. F. P. H., Westendorp, R. G. J., Hack, C. E., & Sturk, A. (2000). Cellular origin and procoagulant properties of microparticles in meningococcal sepsis. *Blood*, *95*(3), 930–935.

O'dea, K. P., Porter, J. R., Tirlapur, N., Katbeh, U., Singh, S., Handy, J. M., & Takata, M. (2016). Circulating microvesicles are elevated acutely following major burns injury and associated with clinical severity. *Plos One*, *11*(12), e0167801. https://doi.org/10.1371/journal.pone.0167801

Porro, C., Lepore, S., Trotta, T., Castellani, S., Ratclif, L., Battaglino, A., Di Gioia, S., Martínez, M. C., Conese, M., & Maffione, A. B. (2010). Isolation and characterization of microparticles in sputum from cystic fibrosis patients. *Respiratory Research*, *11*, 94. https://doi.org/10.1186/1465-9921-11-94

Prakash, P. S., Caldwell, C. C., Lentsch, A. B., Pritts, T. A., & Robinson, B. R. H. (2012). Human microparticles generated during sepsis in patients with critical illness are neutrophil-derived and modulate the immune response. *The Journal of Trauma and Acute Care Surgery*, *73*(2), 401–406; discussion 406-407. https://doi.org/10.1097/TA.0b013e31825a776d

Salaün, C., James, D. J., & Chamberlain, L. H. (2004). Lipid rafts and the regulation of exocytosis. *Traffic*, *5*(4), 255–264. https://doi.org/10.1111/j.1600-0854.2004.0162.x

Sarlon-Bartoli, G., Bennis, Y., Lacroix, R., Piercecchi-Marti, M. D., Bartoli, M. A., Arnaud, L., Mancini, J., Boudes, A., Sarlon, E., Thevenin, B., Leroyer, A. S., Squarcioni, C., Magnan, P. E., Dignat-George, F., & Sabatier, F. (2013). Plasmatic level of leukocyte-derived microparticles is associated with unstable plaque in asymptomatic patients with high-grade carotid stenosis. *Journal of the American College of Cardiology*, *62*(16), 1436–1441. https://doi.org/10.1016/j.jacc.2013.03.078

Skryabin, G. O., Komelkov, A. V., Savelyeva, E. E., & Tchevkina, E. M. (2020). Lipid rafts in exosome biogenesis. *Biochemistry (Moscow)*, *85*(2), 177–191. https://doi.org/10.1134/s0006297920020054

Soni, S., Garner, J. L., O'dea, K. P., Koh, M., Finney, L., Tirlapur, N., Srikanthan, K., Tenda, E. D., Aboelhassan, A. M., Singh, S., Wilson, M. R., Wedzicha, J. A., Kemp, S. V., Usmani, O. S., Shah, P. L., & Takata, M. (2020). Intra-alveolar neutrophil-derived microvesicles are associated with disease severity in COPD. *American Journal of Physiology. Lung Cellular and Molecular Physiology*, Published online November 4, https://doi.org/10.1152/ajplung.00099.2020

Stiel, L., Delabranche, X., Galoisy, A.-C., Severac, F., Toti, F., Mauvieux, L., Meziani, F., & Boisramé-Helms, J. (2016). Neutrophil fluorescence: A new indicator of cell activation during septic shock-induced disseminated intravascular coagulation. *Critical Care Medicine*, *44*(11), e1132–e1136. https://doi.org/10.1097/CCM.0000000000001851

Suades, R., Padró, T., Crespo, J., Sionis, A., Alonso, R., Mata, P., & Badimon, L. (2019). Liquid biopsy of extracellular microvesicles predicts future major ischemic events in genetically characterized familial hypercholesterolemia patients. *Arteriosclerosis, Thrombosis, and Vascular Biology*, *39*(6), 1172–1181. https://doi.org/10.1161/ATVBAHA.119.312420

Théry, C., Witwer, K. W., Aikawa, E., Alcaraz, M. J., Anderson, J. D., Andriantsitohaina, R., Antoniou, A., Arab, T., Archer, F., Atkin-Smith, G. K., Ayre, D. C., Bach, J.-M., Bachurski, D., Baharvand, H., Balaj, L., Baldacchino, S., Bauer, N. N., Baxter, A. A., Bebawy, M., … Zuba-Surma, E. K. (2018). Minimal information for studies of extracellular vesicles 2018 (MISEV2018): A position statement of the International Society for Extracellular Vesicles and update of the MISEV2014 guidelines. *Journal of Extracellular Vesicles*, *7*(1), 1535750. https://doi.org/10.1080/20013078.2018.1535750

Timár, C. I., Lőrincz, Á. M., Csépányi-Kömi, R., Vályi-Nagy, A., Nagy, G., Buzás, E. I., Iványi, Z., Kittel, Á., Powell, D. W., Mcleish, K. R., & Ligeti, E. (2013). Antibacterial effect of microvesicles released from human neutrophilic granulocytes. *Blood*, *121*(3), 510–518. https://doi.org/10.1182/blood-2012-05-431114

Tomar, B., Anders, H. J., Desai, J., & Mulay, S. R. (2020). Neutrophils and neutrophil extracellular traps drive necroinflammation in COVID-19. *Cells*, *9*(6), 1383. https://doi.org/10.3390/cells9061383

Van Avondt, K., & Hartl, D. (2018). Mechanisms and disease relevance of neutrophil extracellular trap formation. *European Journal of Clinical Investigation*, *48*(Suppl 2), e12919. https://doi.org/10.1111/eci.12919

Van Deun, J., Mestdagh, P., Agostinis, P., Akay, Ö., Anand, S., Anckaert, J., Martinez, Z. A., Baetens, T., Beghein, E., Bertier, L., Berx, G., Boere, J., Boukouris, S., Bremer, M., Buschmann, D., Byrd, J. B., Casert, C., Cheng, L., Cmoch, A., … Hendrix, A. (2017). EV-TRACK: transparent reporting and centralizing knowledge in extracellular vesicle research. *Nature Methods*, *14*(3), 228–232. https://doi.org/10.1038/nmeth.4185

Varela-Eirin, M., Varela-Vazquez, A., Rodríguez-Candela Mateos, M., Vila-Sanjurjo, A., Fonseca, E., Mascareñas, J. L., Eugenio Vázquez, M., & Mayan, M. D. (2017). Recruitment of RNA molecules by connexin RNA-binding motifs: Implication in RNA and DNA transport through microvesicles and exosomes. *Biochimica Et Biophysica Acta*, *1864*(4), 728–736. https://doi.org/10.1016/j.bbamcr.2017.02.001

Wang, J., Li, Q., Yin, Y., Zhang, Y., Cao, Y., Lin, X., Huang, L., Hoffmann, D., Lu, M., & Qiu, Y. (2020). Excessive neutrophils and neutrophil extracellular traps in COVID-19. *Frontiers in Immunology*, *11*, 2063. https://doi.org/10.3389/fimmu.2020.02063

Welsh, J. A., Van Der Pol, E., Arkesteijn, G. J. A., Bremer, M., Brisson, A., Coumans, F., Dignat-George, F., Duggan, E., Ghiran, I., Giebel, B., Görgens, A., Hendrix, A.n, Lacroix, R., Lannigan, J., Libregts, S. F. W. M., Lozano-Andrés, E., Morales-Kastresana, A., Robert, S., De Rond, L., Tertel, T., & Jones, J. C. (2020). MIFlowCyt-EV: A framework for standardized reporting of extracellular vesicle flow cytometry experiments. *Journal of Extracellular Vesicles*, *9*(1), 1713526. https://doi.org/10.1080/20013078.2020.1713526

Yáñez-Mó, M., Siljander, P. R.-M., Andreu, Z., Bedina Zavec, A., Borràs, F. E., Buzas, E. I., Buzas, K., Casal, E., Cappello, F., Carvalho, J., Colás, E., Cordeiro-Da Silva, A., Fais, S., Falcon-Perez, J. M., Ghobrial, I. M., Giebel, B., Gimona, M., Graner, M., Gursel, I., … De Wever, O. (2015). Biological properties of extracellular vesicles and their physiological functions. *Journal of Extracellular Vesicles*, *4*(1), 27066. https://doi.org/10.3402/jev.v4.27066

Zuo, Y., Zuo, M., Yalavarthi, S., Gockman, K., Madison, J. A., Shi, H., Woodard, W., Lezak, S. P., Lugogo, N. L., Knight, J. S., & Kanthi, Y. (2021). Neutrophil extracellular traps and thrombosis in COVID-19. *Journal of Thrombosis and Thrombolysis*, *51*(2), 446–453. https://doi.org/10.1007/s11239-020-02324-z

Zwaal, R. F., & Schroit, A. J. (1997). Pathophysiologic implications of membrane phospholipid asymmetry in blood cells. *Blood*, *89*(4), 1121–1132.

SUPPORTING INFORMATION

Additional supporting information may be found in the online version of the article at the publisher's website.

How to cite this article: Bonifay, A., Robert, S., Champagne, B., Petit, P.-R., Eugène, A., Chareyre, C., Duchez, A.-C., Vélier, M., Fritz, S., Vallier, L., Lacroix, R., & Dignat-George, F. (2022). A new strategy to count and sort neutrophil-derived extracellular vesicles: Validation in infectious disorders. *Journal of Extracellular Vesicles*, *11,* e12204. https://doi.org/10.1002/jev2.12204